Morphology and Gas Adsorption Properties of Palladium−Cobalt-Based Cyanogels

Rahul S. Deshpande, Stefanie L. Sharp-Goldman, Jennifer L. Willson, and Andrew B. Bocarsly*

Department of Chemistry, Frick Laboratory, Princeton University, Princeton, New Jersey 08544

Joachim Gross†

Department of Civil Engineering, Princeton University, Princeton, New Jersey 08544

Adam C. Finnefrock and Sol M. Gruner

Cornell High Energy Synchrotron Source (CHESS), Cornell University, Ithaca, New York 14853

Received March 31, 2003. Revised Manuscript Received August 6, 2003

The morphology of cyanide-bridged palladium−cobalt (Pd−Co) gels, synthesized from aqueous solutions of Na_2PdCl_4 and $K_3[Co(CN)_6]$, is elucidated using nitrogen and carbon dioxide adsorption, permeability measurements, electron microscopy, and small-angle X-ray scattering. The aerogels formed from the Pd−Co hydrogels possess both micro- and mesoporosity. Electron microscopy indicates that the aerogels are constituted of spherical microporous particles; the interstices between these particles constitute the mesopores. The aerogel surfaces are found to be fractal as analyzed by gas adsorption and small-angle X-ray scattering. Both these techniques yield, within experimental error, the same surface fractal dimension of 2.6 ± 0.2 for the aerogels. The Pd−Co xerogels, unlike the aerogels, are predominantly microporous with a narrow microporosity. Transmission electron microscopy reveals that the xerogels are constituted of particles of an average size of ∼10 nm. Unlike the aerogels, the xerogels do not possess surface fractality. The mechanism of adsorption of different gases on these gels is analyzed on the basis of the gel morphologies.

Introduction

In recent years, considerable research activity has been directed toward the synthesis of porous materials using sol−gel techniques.[1] These materials have important applications in diverse areas such as heterogeneous catalysis, selective adsorption, and shape-selective molecular sieving. The sol−gel technique offers a remarkable ability to tailor the properties of these porous materials by manipulating those of their precursors.[1,2] The ability to tailor materials is enhanced by a knowledge of the surface and bulk morphology of the porous materials.

We have previously reported[3] that aqueous solutions of the square planar complex, Na_2PdCl_4 and $K_x[M(CN)_n]$ − with $n = 4-8$ and M is a transition metal − react to form gelled polymeric systems via the reaction

$$2x\,[PdCl_4]^{2-} + x[M(CN)_6]^{n-} \rightarrow [(CN)_4M(CN)_2\,\{\text{trans-}PdCl_2\}_2]_x^{n-} + 4x\,Cl^- \quad (1)$$

The product polymer is characterized by the presence of bridging cyanide ligands between the Pd(II) and M metal centers, forming a star-polymer system.[4] Polymerization occurs via the substitution of two chloride ligands, trans to each other, on the Pd(II) centers, by the nitrogen end of the cyanide ligands on M metal center, to generate an extended cyanide-bridged structure. Because the cyanide bridges are central to these gels and distinguish them from classic metal−oxo gels, we refer to these gels, generically, as cyanogels.

The hydrogels obtained on mixing the aqueous transition metal reagent solutions are typically ∼95% water by mass. From these, aero- or xerogels are obtained depending on the solvent removal process employed. A supercritical extraction of the solvent yields the aerogel, whereas the xerogel is obtained by direct evaporation of the solvent close to its boiling point and ambient pressure.[5] We have established that these cyanogels are

* Corresponding author. Phone: (609) 258-3888. E-mail: bocarsly@princeton.edu.

† Current address: Zentrum fuer Medizinische Forschung, Sektion Minimal Invasive Chirurgie, Waldhoernlestr. 22, D-72072 Tuebingen Germany.

(1) Brinker, C. J.; Scherer, G. W. *Sol Gel Science*: *The Physics and Chemistry of Sol−Gel Processing*; Academic Press: Boston, 1990.

(2) Barton, T. J.; Bull, L. M.; Klemperer, W. G.; Loy, D. A.; McEnaney, B.; Misono, M.; Monson, P. A.; Pez, G.; Scherer, G. W.; Vartuli, J. C.; Yaghi, O. M. *Chem. Mater.* **1999**, *11*, 2633.

(3) Pfennig, B. W.; Bocarsly, A. B.; Prud'homme, R. K. *J. Am. Chem. Soc.* **1993**, *115*, 2661.

(4) Heibel, M. *Sol−Gel Chemistry of the New Inorganic Polymers − Cyanogels*. Ph.D. Thesis, University of Ljubljana, Ljubljana, Slovenia, 1996.

(5) Sharp, S. L. *The Physical Characterization and Sol−Gel Chemistry of the Cyanogel System*. Ph.D. Thesis, Princeton University, Princeton, NJ, 2000.

10.1021/cm034216m CCC: $25.00
Published on Web 10/03/2003

highly porous systems[6] with a high specificity for CO_2[7] over other single gas-phase species.

In this paper, we probe the morphology and topology of palladium−cobalt based cyanogels synthesized by the sol−gel technique. Nitrogen and carbon dioxide adsorption, electron microscopy, permeability measurements, and small-angle X-ray scattering are among the techniques used for the elucidation of the gel morphologies. The data obtained indicate that the palladium−cobalt-based aerogels are composed of spherical particles with fractal surfaces.

Such fractally rough gels containing palladium and cobalt metal centers may have important applications in heterogeneous catalysis, as catalytic activity[8] and transport efficiency[9] often are related to surface self-similarity. In addition, the presence of narrow micro- and mesoporosity in these gels makes them suitable candidates for selective gas adsorbents and filters.

Experimental Section

The gels studied in this paper were synthesized from aqueous solutions of sodium tetrachloropalladate(II), Na_2PdCl_4, and potassium hexacyanocobaltate(III), $K_3[Co(CN)_6]$, in a 2:1 molar ratio, respectively, at room temperature. The starting chemicals were reagent grade: the former was obtained from Pressure Chemicals Inc. and the latter was from Aldrich Inc. Both were used as received. In-house deionized, osmotically purified water was used for all the solutions.

A typical hydrogel was synthesized by a 2:1 volumetric reaction between 0.4 M solutions of Na_2PdCl_4 and $K_3[Co(CN)_6]$ which provides a stoichiometric ratio.[3] Such a gel is referred to as a 0.4 M Pd−Co cyanogel. The resulting mixed solution was poured into tubular glass molds (with an inner diameter of 12.5 mm) to facilitate further handling of the gels. Mixing the reactants together resulted in a dark orange colored solution that, over time, increased in viscosity. This solution underwent a well-defined sol−gel transition, and polymeric gel beams, consisting of cyanide-bridged palladium−cobalt centers, formed between the walls of the molds. Thermogravimetric analysis of the hydrogel revealed that it was composed of 99% water immediately on formation and eventually stabilized at ∼95% water.[3] The orange gel beam samples were allowed to age for one week at 9 °C in the glass molds. During this time the gel beam dimensions decreased by ∼ 15%, allowing them to be easily removed from the molds. After their removal, they were placed in a deionized water bath at room temperature. The water was changed daily for approximately 4 d to remove the product potassium chloride from the gel beams. When the addition of a 0.5 M silver nitrate solution to the bath no longer formed a precipitate, indicating no free chloride, this treatment was suspended. The gel beams produced were generally 70−80 mm long and 10−10.5 mm in diameter.

Aerogels were made from these gel beams by, first, placing them in an acetone bath to exchange the water with acetone. The bath was changed twice daily for 3 d to ensure that all the water in the gel beams was replaced by acetone. The acetone-impregnated beams were then placed in a computer-controlled autoclave (CF Technologies, CFT-AD-50, 600 mL volume), and the acetone was exchanged with CO_2 (BOC gases, 99.99% purity). The autoclave was flushed five times with liquid CO_2 to ensure a complete exchange of acetone with CO_2. It was then brought up to 1300 psi and 45 °C to render the CO_2 supercritical; the supercritical CO_2 was then carefully released. The autoclave was subsequently brought to ambient pressure. Xerogels were made by smearing out the hydrogels on a filter paper to eliminate the water. These were subsequently dried overnight in an oven at 95 °C. The resulting xerogels were rinsed with distilled water to remove the salts produced during the reaction, dried again in the oven, and then mechanically powdered.

Ar (99.9%), CH_4 (99.9%), CO_2 (99.99%), N_2 (99.9%), and O_2 (99.9%) were obtained from BOC gases, and N_2O (99%) and SF_6 (99.75%) were obtained from Aldrich. All gases were used as received. Electron microscopic imaging of the gels was accomplished with a Philips XL30 FEG Scanning Electron Microscope. Small-angle X-ray Scattering (SAXS) was performed at Cornell University's CHESS facility. The X-ray wavelength was selected with a multilayer monochromator tuned to $\lambda = 1.41$ Å and then imaged with an in-house 2K × 2K CCD detector. Exposure times for each image ranged from 10 to 100 s, with up to 20 exposures acquired for each sample to improve the dynamic range of the scattering data. The q-dimension of each image was calibrated with silver behenate ($d = 58.376$ Å) and silica sphere (R = 278 Å) references.[10,11] Images from each sample were summed, the background was subtracted, and the intensity and distortion were corrected. The resulting images were azimuthally averaged to produce the intensity profile.[12] All reported data have been *t*-tested. The N_2 adsorption isotherms were measured at −196 °C, and the ones with CO_2 were recorded at 0 °C, both in the pressure range 14.7×10^{-6} to 16 psi. The specific surface area was calculated using the Brunauer−Emmett−Teller (BET) model[13] using data in the 0.06−0.3 relative pressure range. Pore size distributions (PSD) for the studied samples were computed using the Barrett−Joyner−Halenda (BJH) method[14] applied to the desorption branch of the nitrogen isotherm. The microporosity of the samples was assessed by using the *t*-plot method.[15] An empirical Harkins−Jura adsorption isotherm was used to represent an isotherm on a nonporous reference adsorbent. Thermogravimetric analyses were recorded with a Perkin-Elmer TGA-7 under an argon atmosphere on degassed samples. Nitrogen and carbon dioxide adsorption data were collected on a Micromeritics ASAP 2010.

Warning: Hazardous gases, HCN and $(CN)_2$, can be evolved during the heating of the gels above 200 °C. Therefore, while doing the thermogravimetric analyses, it is important to trap all product gases using a series of bubblers: the first one should contain bleach and the terminal one should contain sodium hydroxide.

Results and Discussion

Adsorption of Different Gases by the Cyanogels. Figure 1 shows the gravimetric profile of the adsorption of pure CO_2 on a powdered sample of 60 mM Pd−Co xerogel. Argon was used to desorb the adsorbed CO_2. The pressures of both the gases were kept constant at 20 psi. As this figure illustrates, the xerogel adsorbs about 4% of CO_2 by mass and the adsorption is completely reversible at 25 °C. Although Figure 1 shows only three CO_2−Ar cycles, this cycling was carried out 10 times with almost no change, indicating the reproducibility and complete reversibility of CO_2 adsorption on the xerogels.

(6) Sharp, S. L.; Bocarsly, A. B.; Scherer, G. W. *Chem. Mater.* **1998**, *10*, 825.
(7) Deshpande, R. S.; Sharp-Goldman, S. L.; Bocarsly, A. B. *Langmuir* **2002**, *18*, 7694.
(8) Rigby, S. P.; Gladden, L. F. *J. Catal.* **1998**, *180*, 44.
(9) Conner, W. C.; Bennett, C. O. *J. Chem. Soc., Faraday Trans.* **1993**, *89*, 4109.
(10) Blanton, T. N.; Huang, T. C.; Toraya, H.; Hubbard, C. R.; Robie, S. B.; Louer, D.; Goebel, H. E.; Will, G.; Gilles, R.; Raferty, T. *Powder Diffr.* **1995**, *10*, 91.
(11) Megens, M.; van Kats, C. M.; Beosecke, P.; Vos, W. L. *Langmuir* **1997**, *13*, 6120.
(12) Bergna, H. E. *The Colloidal Chemistry of Silica*; American Chemical Society: Washington, DC, 1994.
(13) Brunauer, S.; Emmett, P. H.; Teller, E. *J. Am. Chem. Soc.* **1938**, *60*, 0, 309.
(14) Barett, E. P.; Joyner, L. G.; Halenda, P. H. *J. Am. Chem. Soc.* **1951**, *73*, 373.
(15) Gregg, S. J.; Sing, K. S. W. *Adsorption, Surface Area and Porosity*; 2nd ed.; Academic Press: London, 1982.

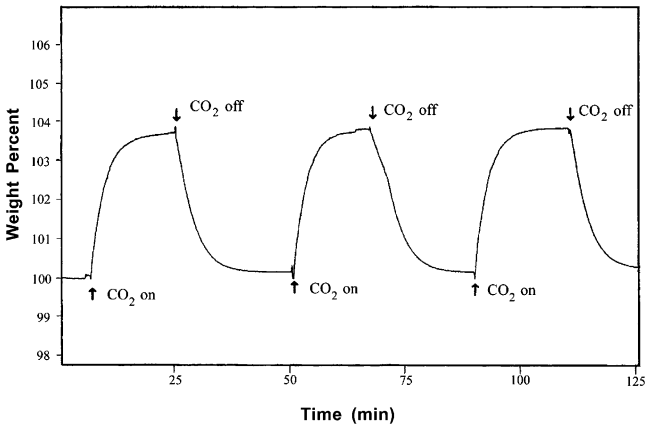

Figure 1. Carbon dioxide−argon recycling data for the 60 mM xerogel system illustrating the complete reversibility and reproducibility of CO_2 adsorption. Although the figure shows only three CO_2−Ar cycles, this cycling was carried out 10 times with almost no change, indicating the reproducibility and the complete reversibility of CO_2 adsorption.

The Pd−Co aerogels show a similar adsorption profile; however, they take up about 9% by mass of CO_2. The adsorption of N_2O by the gels is identical to that of CO_2 in terms of the amount of the gas adsorbed. The increased gas adsorption by the aerogels is in line with their larger mean pore size[7] and expanded structure vis-à-vis the xerogels. Another indication of the smaller pore dimensions of the xerogels is provided by the fact that no detectable SF_6 adsorption is observed on the xerogels; the aerogels, in contrast, take up 11% of SF_6 by mass. Neither of the gels adsorbs Ar, N_2, O_2, or CH_4 under ambient conditions: these gases, therefore, are suitable candidates for desorbing the adsorbed gases off the gels.

Porosity of the Cyanogels. *Microporosity of the Pd−Co Xerogels.* Figure 2 shows the N_2 and CO_2 adsorption isotherms measured at −196 °C and 0 °C, respectively, for both the 0.4 M aero- and xerogels. The xerogel isotherm is shown in Figure 2(a) and Figure 2(b) depicts that for the aerogel. The xerogel shows a distinct Type I isotherm[15] indicating that it is almost purely microporous. The aerogel, on the other hand, yields a Type IV isotherm,[15] characteristic of a mesoporous solid.

The pore size distribution (PSD) in the cyanogels is shown in Figure 3. Figure 3(a) depicts the PSD plot for the 0.4 M Pd−Co xerogel obtained by applying the Saito Foley-extended Horvath Kawazoe (HK) model to the nitrogen adsorption data for the xerogel. As can be observed, the pore diameters in the xerogel lie in the sub-2 nm range with a peak at 0.9 nm indicative of its microporous nature.

Figure 4(a) and (b) clearly illustrate the N_2 and the CO_2 adsorption isotherms, respectively, for both the 0.4 M Pd−Co aerogel and xerogel in the low relative pressure regime. As can be seen, in this region the N_2 and the CO_2 adsorption isotherms for both the gels are curved. It has been shown[16] that curved isotherms in the low relative pressure region are obtained from materials consisting of narrow micropores—i.e., possessing a narrow microporosity—whereas wide microporosity leads to more linear isotherms in the low relative pressure region. Curved isotherms are associated with

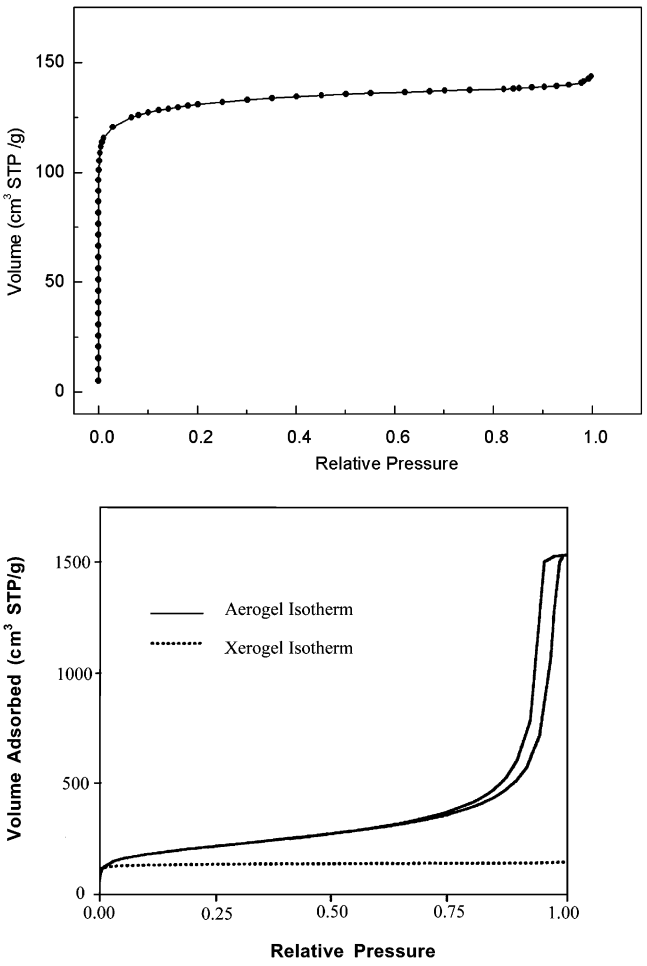

Figure 2. (a) Nitrogen adsorption isotherm at 77 K for the 0.4 M Pd−Co xerogel. The classic Type I isotherm indicates that the xerogel is almost predominantly microporous. (b) Nitrogen adsorption and desorption isotherms obtained at 77 K for the 0.4 M aerogel and xerogel. The volume adsorbed by the aerogel is an order of magnitude greater than that for the xerogel.

enhanced adsorption potential in micropores smaller than two molecular diameters of CO_2.[16] In such narrow pores, the potential fields from the neighboring walls overlap significantly, thereby enhancing the interaction potential between the pore walls and the adsorbate molecules.[17−19] This enhanced interaction leads to a curvature of the adsorption isotherm as a large amount of the adsorbate is adsorbed at very low relative pressures. The steep initial part of the xerogel isotherm, indicating that >75% of the pore volume is filled at $p <$ 0.1 atm, is a manifestation of the high fields present within these micropores. Additional evidence for the narrow microporosity in the xerogel comes from the difference in the values of the xerogel pore volumes obtained on applying the Dubinin−Radushkevich[20] (DR) equation to the N_2 and CO_2 adsorption data. Table 1 lists these values as well as those of surface areas

(16) Martin-Martinez, J. M.; Mittelmeijer-Hazeleger, M. C. *Langmuir* **1993**, *9*, 3317.

(17) Everett, D. H.; Powl, J. C. *J. Chem. Soc., Faraday Trans.* **1976**, *72*, 619.

(18) Maitland, G. C.; Rigby, M.; Smith, E. B.; Wakeham, W. A. *Intermolecular Forces*: *Their Origin and Determination*; Clarendon: Oxford, 1981.

(19) Steele, W. A. *The Interactions of Gases with Solid Surfaces*; Pergamon: Oxford, 1973.

(20) Dubinin, M. M.; Radushkevich, L. V. *Proc. Acad. Sci. USSR* **1947**, *55*, 331.

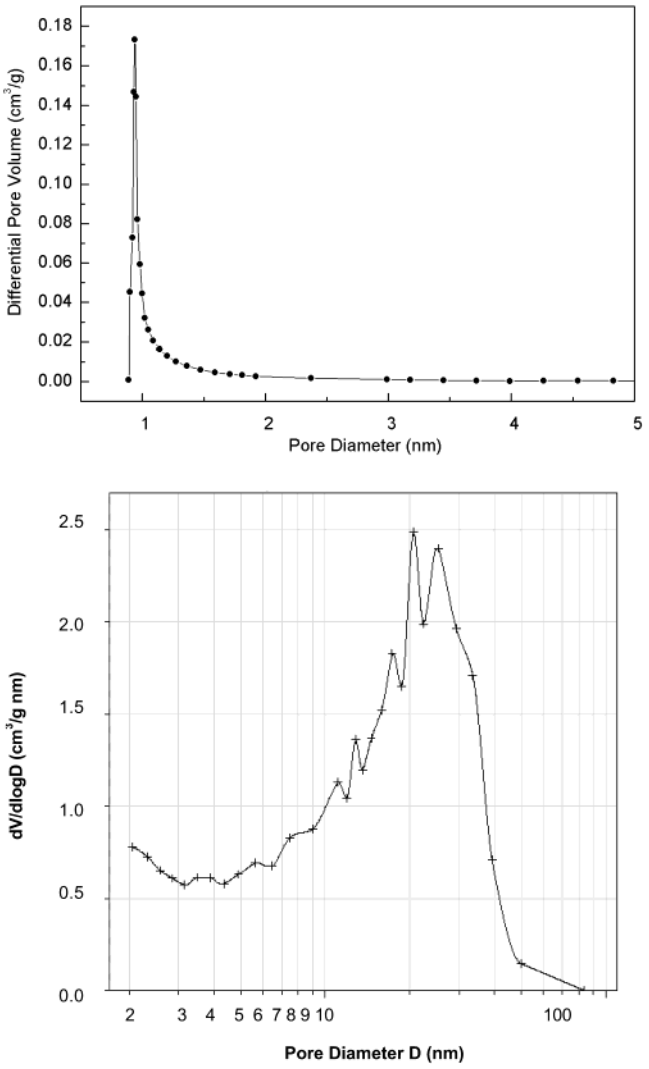

Figure 3. (a) Pore size distribution plot for the 0.4 M Pd−Co xerogel indicative of its microporous nature. The plot has been made using the Saito−Foley extended Horvath Kawazoe model. (b) BJH plot for the 0.4 M Pd−Co aerogel showing the presence of mesopores.

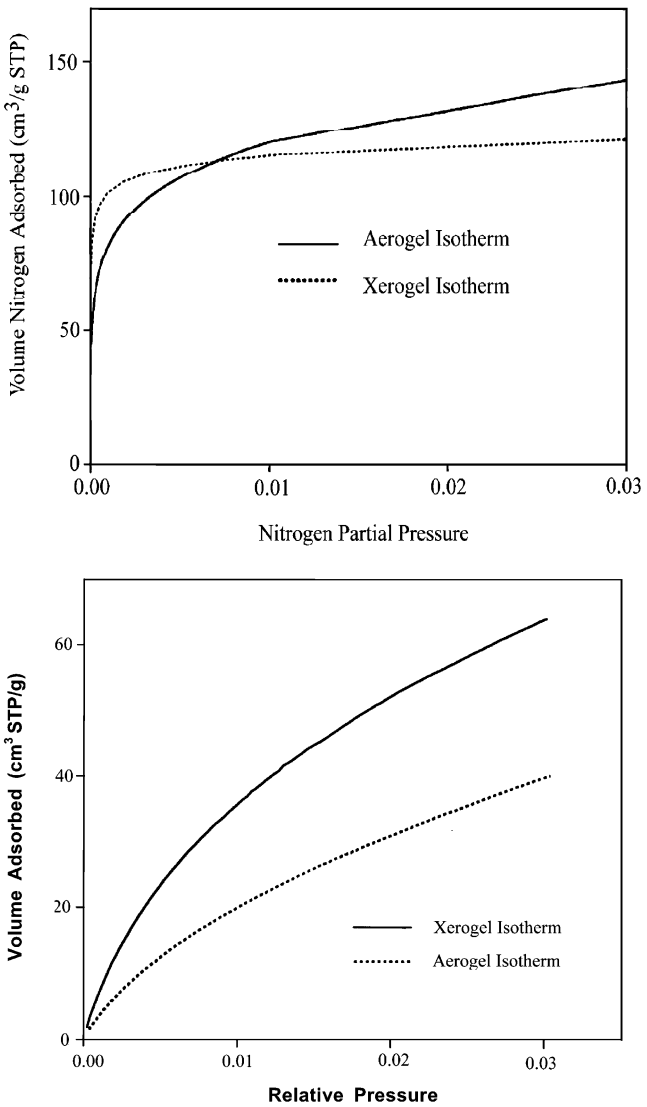

Figure 4. (a) Close-up of the N_2 adsorption isotherm in the low partial pressure region illustrating the curved isotherms indicative of narrow microporosity for both the 0.4 M aero- and xerogel. (b) CO_2 adsorption isotherms obtained at 273 K for both the 0.4 M aero- and xerogel in the low partial pressure region. The curvature of the isotherms is characteristic of narrow microporosity in these gels.

obtained on the application of the Brunauer, Emmett, and Teller[13] (BET) model to the adsorption data for the 0.4 M Pd−Co xerogel. In systems with narrow microporosity, the diffusion of N_2 molecules in narrow micropores at −196 °C is kinetically restricted. No such barrier exists for CO_2 molecules, as the adsorption takes places at 0 °C.[21] Hence, in microporous materials, the application of the DR equation to the CO_2 adsorption data leads to a larger pore volume vis-à-vis that obtained from the N_2 adsorption data. Both these observations—the curved adsorption isotherms in the low relative pressure regime and the difference in the micropore volumes obtained from the N_2 and CO_2 adsorption data—clearly indicate that the pores in the xerogel are exceedingly narrow, i.e., the xerogel possesses a narrow microporosity. Transmission electron microscope imaging of the Pd−Co xerogels, Figure 5, leads to the conclusion that the average particle size in the xerogels is ∼10 nm.

Dual Porosity of the Aerogels. Unlike the predominantly microporous xerogel, the aerogel possesses both micro- and mesoporosity. Figure 3(b) displays the PSD plot for the 0.4 M Pd−Co aerogel obtained by the application of the BJH model to the desorption branch of the nitrogen isotherm on the aerogel. It indicates that the pore diameters in the aerogels range from 3 to 40 nm implying that the Pd−Co aerogel is primarily mesoporous. A pronounced uptake in the low relative pressure region—as Figure 4(a) and (b) shows—implies the existence of micropores in the aerogel. The curved nature of the isotherms in this pressure region, together with the difference in the pore volume values calculated from the DR equation applied to the N_2 and CO_2 adsorption data, as shown in Table 1, point to the existence of narrow microporosity within the aerogel. Table 1 lists the adsorption data for the 0.4 M Pd−Co aerogel primarily because the adsorption data for other aerogels studied in this paper are similar. Additionally, in our earlier studies,[6] it has been observed that

(21) Garrido, J.; Linares-Solano, A.; Martin-Martinez, J. M.; Molina-Sabio, M.; Rodriguez-Reinoso, F.; Torregrosa, R. *Langmuir* **1987**, *3*, 76.

Table 1. Surface Areas and Micropore Volumes of the 0.4 M Pd−Co Cyanogels

sample	N_2-S_{BET}[a] (m^2/g)	N_2-S_{DR}[b] (m^2/g)	CO_2-S_{DR}[b] (m^2/g)	N_2-V_p[c] (cm^3/g)	N_2-V_{DR}[d] (cm^3/g)	CO_2-V_{DR}[d] (cm^3/g)
0.4 M aerogel	730.71 ± 3.29	450.62 ± 3.17	822.82 ± 5.14	2.37 ± 0.17	0.23 ± 0.05	0.26 ± 0.05
0.4 M xerogel	439.36 ± 4.17	491.78 ± 3.84	705.11 ± 4.93	0.22 ± 0.07	0.19 ± 0.04	0.28 ± 0.06

[a] N_2-S_{BET}. Total surface area determined by applying the Brunauer−Emmett−Teller (BET) equation to the nitrogen adsorption data. [b] N_2-S_{DR} and CO_2-S_{DR}. Surface area of the micropore region determined by applying the Dubinin−Radushkevich equation to the nitrogen and carbon dioxide adsorption data. [c] N_2-V_p. Total pore volume determined by measuring the volume of nitrogen absorbed at the saturation pressure of N_2. [d] N_2-V_{DR} and CO_2-V_{DR}. Micropore pore volume determined by applying the Dubinin−Radushkevich equation to the nitrogen and carbon dioxide adsorption data.

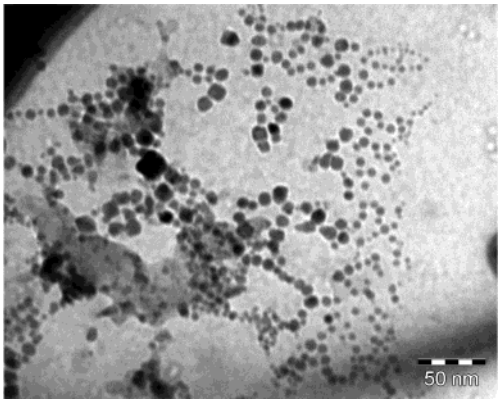

Figure 5. Transmission electron microscope image of a 0.4 M Pd−Co xerogel. The particle size averages ∼10 nm.

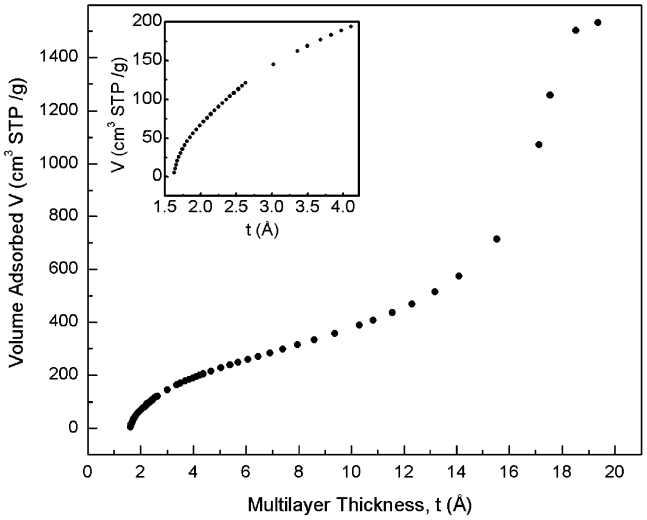

Figure 6. *t*-Plot for the 0.4 M Pd−Co aerogel showing both the mesoporosity and the microporosity (inset). The pronounced curvature in the low-*t* region (inset) is indicative of microporosity in the aerogel.

although the mean pore radius in the Pd−Co cyanogels is highly sensitive to the gel concentration, the porosity is very weakly dependent on gel concentration: it varies by less than 5% when the concentration is varied by a factor of 5. The final evidence for microporosity in Pd−Co aerogels is provided by the *t*-plot analysis of the aerogel isotherm. Figure 6 shows the *t*-plot for the 0.4 M Pd−Co aerogel. The curvature in the *t*-plot in the region of low *t* values clearly attests to the presence of microporosity in the Pd−Co aerogels.

Unlike the N_2 adsorption isotherm for the xerogel, which is of Type I, the N_2 adsorption isotherm for the 0.4 M Pd−Co aerogel is a type IV isotherm,[15] characteristic of a mesoporous solid (cf. Figure 2(b)). The isotherm displays hysteresis: the H1 hysteresis loop is

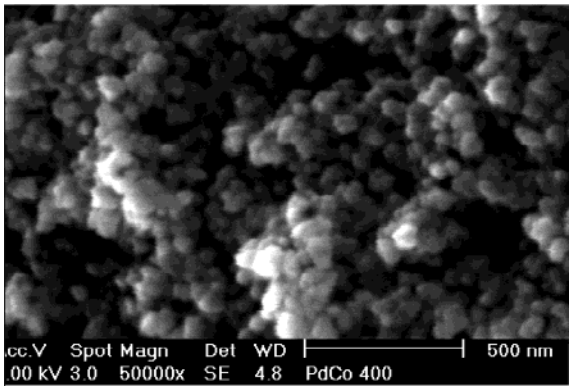

Figure 7. Scanning electron micrograph of a 0.4 M Pd−Co aerogel illustrating the "packed cotton ball" model. The "packed cotton ball" refers to the micropore-containing aerogel particles that, on average, are ∼40 nm in diameter. The interstitial voids that arise from packing of these aerogel particles constitute the mesopores.

Table 2. Comparison of Sorption Data, Beam Bending Data, and Calculated Estimates

type of measurement performed on aerogel	density of aerogel (g/cm^3)	mean pore radius[a] within aerogel (nm)	total pore volume of aerogel (cm^3/g)
permeability measurement	0.10 ± 0.02	17.1 ± 1.8	9.36 ± 1.83
nitrogen sorption experiment		6.48 ± 1.28	2.37 ± 0.46
calculated values due to N_2 sorption shrinkage	0.28 ± 0.05	5.98 ± 1.17	3.08 ± 0.55

[a] Mean pore radius found from the nitrogen sorption experiment was determined by (2 × volume of N_2 adsorbed)/(BET surface area).

characteristic of capillary condensation in mesopores. Such a loop is often obtained with agglomerates or compacts of spherical particles of fairly uniform size and is typical of aerogels.[15]

Scanning electron microscope images of the 0.4 M aerogel, Figure 7, indicate that it is composed of spherical particles of 40 ± 3 nm in diameter. The mean pore radius calculated from the three-point beam bending measurements[6] is 17.1 ± 1.8 nm. This value is in sharp contradiction with the mean pore radius calculated from the N_2 desorption which yields a significantly smaller pore radius of 6.48 ± 1.28 nm. Table 2 lists the values of mean pore radius and pore volume obtained through different techniques. The discrepancy between the pore values obtained from the N_2 adsorption and from beam-bending measurements is not surprising because gas adsorption is expected to significantly deform the shape and size of pores in these compliant aerogels. As the liquid adsorbate begins to desorb from the pores, high capillary pressure gradients[22] that are

strong enough to cause a substantial contraction of a material as fragile and compliant as an aerogel,[23] are generated in the pores. These deformations are especially pronounced during desorption of the capillary condensate from the mesopores of the aerogels. Hence, the data obtained from the gas adsorption relate to the pore sizes in the deformed aerogels, whereas those obtained from the three-point beam-bending measurements pertain to the pore sizes in pristine hydrogels. The beam bending measurements lead, inter alia, to the values of the elastic modulus and permeability of the hydrogel network. It has been shown[22] that in the case of fragile and compliant aerogels, the true pore size and pore volume can be estimated from knowledge of the elastic modulus of the gel network.

As a result of the probable shrinkage incurred during adsorption, the pore volume determined can be seriously underestimated. However, even though there is some contraction in the pore volume at low relative pressures, the surface area is probably not seriously affected. For instance, it has been demonstrated[24] that a silica aerogel has a comparable surface area before and after being wetted and dried, even though there has been a large change in pore volume. Mercury porosimetry will not give a true pore size either. The aerogels are so compliant that mercury does not enter the pores of the aerogel; instead it compresses the gels.[23]

To have an understanding of the N_2 adsorption data, the maximum shrinkage during desorption (when almost all of the pores are full of liquid) can be determined. The capillary pressure, P_c, exerted on the gel during the measurement can be found from the partial pressure of nitrogen, p/p_o, as[25]

$$P_c = (RT/V_m) \ln(p/p_o) \quad (2)$$

where V_m is the molar volume of liquid nitrogen, T is the absolute temperature, and R is the gas constant. The capillary pressure P_c and the pore radius, r, are related by[26]

$$r = (-b_H RT/P_c V_m)^{1/3} - 2\gamma/P_c \quad (3)$$

where γ is the liquid/vapor interfacial energy and b_H is a constant. For N_2, $V_m = 34.6$ cm^3/g, $b_H = 0.221$, and $\gamma = 8.85$ ergs/cm^2 at $T = 77$ K. Using these parameters eq 3 can be solved. The result can be closely approximated by[22]

$$P_c \approx -(30/r^{1.18}) \quad (4)$$

During desorption, as the relative pressure of nitrogen vapor decreases, the capillary pressure increases in magnitude. The gel network is consequently compressed and it contracts. This contraction leads to an increase in its bulk modulus. The network will stop contracting when the following condition is satisfied:[22]

$$(K_o/m)(\rho_b/\rho_o)^m \approx -[1 - (\rho_b/\rho_s)]P_c \approx [1 - (\rho_b/\rho_s)](30/r^{1.18}) \quad (5)$$

where K_o is the bulk modulus of the gel network, m is a constant related to the power law dependence of the bulk modulus to density, ρ_s is the skeletal density of the gel, ρ_o is the original bulk density, and ρ_b is the final bulk density of the gel at the point when the gel shrinkage stops.

It has been shown that in such gels the pore size varies approximately in proportion to the pore volume[22]

$$r(\rho_b) \approx r(\rho_o)[((1/\rho_b) - (1/\rho_s))/((1/\rho_o) - (1/\rho_s))] \quad (6)$$

The values $r(\rho_b)$ and $r(\rho_o)$ are, respectively, the pore size at maximum compression and the original pore size.

The permeability and moduli of a series of cyanogels were determined previously using a three-point beam bending apparatus.[6] Data obtained through this method on aerogels made from 0.4 M solutions are the following: $K_o = 1.01$ MPa, $m = 2.9$, $\rho_o = 0.102$ g/cm^3, $\rho_s = 2.26$ g/cm^3, and $r = 17.1$ nm. Applying this information to eq 5, it is possible to obtain an estimate of the amount of contraction that the gel system will undergo during adsorption. Equation 5 leads to the solution $\rho_b = 0.269$ g/cm^3; the corresponding pore radius from eq 6 is $r = 5.98$ nm. This compares favorably with the pore radius of 6.48 nm obtained from N_2 desorption.

This indicates that any aerogel with a density less than 0.269 g/cm^3 will contract during nitrogen desorption until its density reaches that value and its pore radius is reduced to ~6 nm. This contraction occurs exclusively during desorption of the capillary condensate, i.e., when the mesopores are being emptied. The micropore volume values, consequently, can be assumed to be accurate. The density predicted for maximum shrinkage is less than that of the xerogel density (1.78 g/cm^3 vs 0.269 g/cm^3), so no contraction is expected in the xerogel system and the gas adsorption values for the xerogel system are valid.

The nitrogen sorption data in conjunction with the previous permeability experiments,[6] lead to the conclusion that there are two levels of porosity in the aerogel system: micropores that can be characterized by nitrogen sorption and mesopores whose true size can be determined by permeability measurements. Scanning electron microscope imaging of the fractured surface of the aerogel reveals globular particles whose packing results in the mesoporous structure of the aerogel system as seen in Figure 7. We propose that the structure of the Pd−Co aerogel can be described as "packed cotton balls". The cotton ball represents the micropore-possessing aerogel particle. For the 0.4 M

(22) Scherer, G. W. *J. Non-Cryst. Solids* **1997**, *215*, 155.
(23) Scherer, G. W.; Smith, D. M.; Stein, D. J. *J. Non-Cryst. Solids* **1995**, *186*, 309.
(24) Johnson, M. F. L.; Ries, H. E., Jr. *J. Am. Chem. Soc.* **1950**, *72*, 4289.
(25) Lowell, S.; Shields, J. E. *Powder Surface Area and Porosity*; Chapman and Hall: New York, 1984.

(26) P_c is related to the pore radius, r, by Laplace's equation:

$$P_c = -2\gamma \cos\theta/(r - t) \quad (1a)$$

where γ is the liquid/vapor interfacial energy, t is the thickness of the adsorbed layer of nitrogen on the pore walls, and θ is the contact angle, generally taken to be zero. The layer thickness can be calculated from the Halsey equation:

$$t = (-b_H/\ln(p/p_o))^{1/3} \quad (2a)$$

As $\ln(p/p_o) = P_c V_m/RT$ (cf. Equation 2 in the main text), the thickness t is related to the critical pressure P_c by:

$$t = (-b_H RT/P_c V_m)^{1/3} \quad (3a)$$

Substituting this value of t in eq 1a, eq 3 in the main text follows.

aerogel, these spherical particles have an average diameter of 40 ± 3 nm. The interstitial voids between these particles constitute the mesopores of a mean radius of 17.1 ± 1.8 nm. The narrow microporosity within the spheres, as determined by the N_2 sorption experiments, is too small to be picked up by SEM.

With this morphological model of the gels, one can understand the adsorption characteristics of different gases on these gels. CO_2 adsorption takes place in the xerogels primarily by micropore-filling, and by a combination of micropore-filling and capillary condensation in the aerogels. Nitrous oxide is similar to CO_2 in size and is thus adsorbed by the gels in the same manner as CO_2. Consistent with this prediction is the observation that the gravimetric studies on N_2O are similar to those of CO_2. The micropores in the xerogels are too small to permit a detectable adsorption of SF_6.[27] The mesoporous aerogel with its wider pores, in contrast, adsorbs 11% of SF_6 by weight.

Surface Fractality of the Pd−Co Cyanogels. Fractal analysis has become a powerful tool in morphological characterization over the last two decades.[28,29] Fractal surfaces have scale-invariant structural features, i.e., they are self-similar upon changes in resolution. In the fractal paradigm, surface irregularities are treated as an intrinsic property of the surface rather than as a perturbation of the surface that is assumed to be planar.[30] The surface fractal dimension—a number between two and three—is an operative measure of the surface irregularities as well as the space-filling ability of the surface. A higher surface fractal dimension indicates an increased space-filling ability of the given surface.

For investigating the surface fractality of the aerogels, two independent techniques were utilized: nitrogen adsorption at 77 K and small-angle X-ray scattering. In addition to the 0.4 M Pd−Co aerogel, which has been focused on in the earlier part of this paper, three other aerogel concentrations—0.175, 0.5, and 0.8 M—were employed to calculate the surface fractal dimension.

The fractal dimension can be determined in one step from a single adsorption isotherm using a modified Frenkel−Halsey−Hill equation[31]

$$\log V = \text{constant} - (3 - D) \log (\log(p_o/p)) \qquad (7)$$

where V is the adsorbed volume of the adsorbate at STP, p_o and p are the saturation and equilibrium pressures, respectively, and D is the fractal dimension. The above equation holds only when the capillary condensation is taking place.[32]

Figure 8 depicts the log−log plots for the N_2 adsorption data for three aerogel concentrations along with linear least-squares fits of the data to eq 7. It should be noted that the range of relative pressures used for the linear fits varies slightly with the gel concentration, to ensure that the data represent the relative pressure region where capillary condensation takes place. This

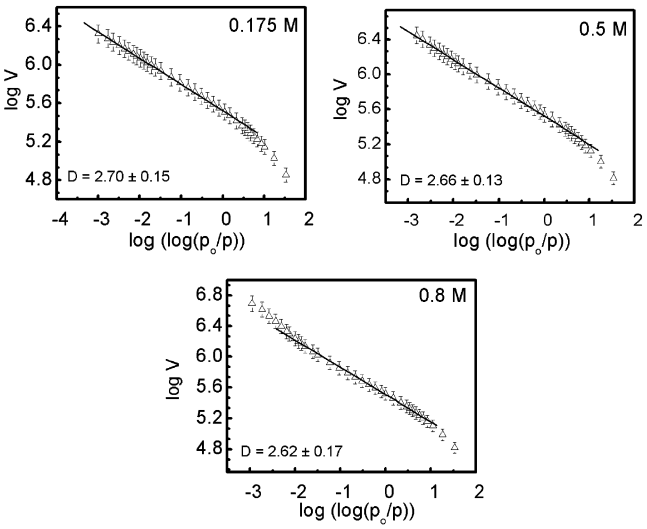

Figure 8. Log−log plots for the N_2 adsorption data for three aerogel concentrations along with the linear least-squares fits to the data. The surface fractal dimension is listed in the bottom left corner of the plots.

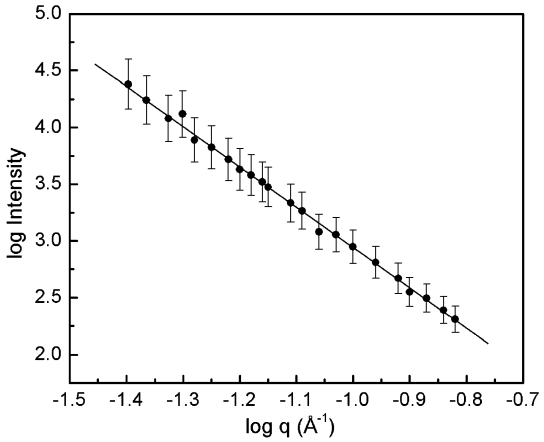

Figure 9. Porod Plot for the 0.4 M Pd−Co aerogel. The surface fractal dimension, D, can be calculated from the slope of the line (cf. text). In this case, D is 2.65 ± 0.14.

condensation is dependent on the mesopore size that, in turn, varies with the gel concentration. As the plots show, the average surface fractal dimension is 2.6 ± 0.2.

Small-angle X-ray scattering experiments were performed on eight Pd−Co aerogel samples: two each of 0.175, 0.4, 0.5, and 0.8 M concentration. Figure 9 illustrates a typical Porod plot for a 0.4 M aerogel. The slope of the linear fit to the data is −3.5 ± 0.2. The slope of the linear fit in a Porod plot represents the mass fractal dimension of a system.[29] The mass and surface fractal dimensions, D_{mf} and D_{sf}, respectively, for a system are related by[29]

$$D_{sf} - D_{mf} = 6 \qquad (8)$$

On the basis of this study, the mass fractal dimension for the Pd−Co aerogels, on average, is −3.3 ± 0.2; therefore, the surface fractal dimension is 2.7 ± 0.2 indicating a nonfractal bulk with a fractal surface. Table 3 compares the surface fractal dimension of the Pd−Co aerogels obtained from the gas-adsorption and small-angle X-ray scattering studies. As it shows, the values of fractal dimension obtained from these two indepen-

(27) Lopez-Ramon, M. V.; Jagiello, J.; Bandosz, T. J.; Seaton, N. A. *Langmuir* **1997**, *13*, 4435.
(28) Pfeifer, P.; Avnir, D.; Farin, D. *J. Chem. Phys.* **1983**, *79*, 3566.
(29) Avnir, D., Ed. *The Fractal Approach to Heterogeneous Chemistry*; John Wiley and Sons: New York, 1989.
(30) Pfeifer, P.; Avnir, D. *J. Chem. Phys.* **1983**, *79*, 3558.
(31) Avnir, D.; Jaroniec, M. *Langmuir* **1989**, *5*, 1431.
(32) Ismail, I. M. K.; Pfeifer, P. *Langmuir* **1994**, *10*, 1532.

Table 3. Surface Fractal Dimension, *D*, of Pd−Co Aerogels by Gas Adsorption and Small-Angle X-ray Scattering (SAXS): A Comparison

aerogel conc. (M)	*D* from gas adsorption	*D* from SAXS
0.175	2.70 ± 0.15	2.72 ± 0.14
0.4	2.67 ± 0.20	2.65 ± 0.14
0.5	2.66 ± 0.13	2.71 ± 0.12
0.8	2.62 ± 0.17	2.67 ± 0.15

dent techniques compare favorably, unambiguously demonstrating the fractal nature of the aerogel surface.

For the xerogel surfaces, the plots of log V vs log(log(p_o/p)) (cf. eq 7) are nonlinear indicating that the xerogels possess nonfractal surfaces. We hypothesize that the difference in the fractal nature of the aerogel and xerogel surfaces may be due to the disparate drying processes used to generate them from the parent hydrogels. High capillary pressure gradients that are encountered in obtaining the xerogels from the hydrogels would be expected to significantly affect their surface properties. Such gradients are absent in aerogel formation. Additionally, it may be anticipated that the prolonged interaction of the hydrogel beams with acetone, that are subsequently used to obtain the aerogels, may have an effect on their surface characteristics. Both these factors would contribute to bringing about a difference in the surface characteristics of the aero- and xerogels that manifests itself in the surface fractal nature of the aerogels.

Conclusions

The palladium−cobalt (Pd−Co) xerogels are predominantly microporous as indicated by both the pore size distribution and the classic Type I isotherm with both N_2 and CO_2. Further, the curved adsorption isotherms in the low relative pressure region with these adsorptives, in conjunction with the disparate pore volume values obtained with N_2 and CO_2 adsorption, point to the narrow microporosity in the Pd−Co xerogel system. The Pd−Co aerogels on the other hand, have a dual porosity. Gas adsorption indicates that they possess micropores—and akin to the xerogels, a narrow microporosity—whereas permeability measurements together with the Type IV adsorption isotherm with an H1 hysteresis loop, enable the conclusion that they are also mesoporous. These data, along with the SEM and SAXS results, lead to the structure of the Pd−Co aerogels as "packed cotton balls". The cotton ball represents the micropore-possessing, surface-fractal aerogel particle. For a 0.4 M aerogel, these particles have an average diameter of 40 ± 3 nm, and the voids between these particles constitute the mesopores of average radius of 17.1 ± 1.8 nm. The adsorption of carbon dioxide and nitrous oxide occurs due to the microporous nature of both the xerogel and the aerogel, whereas SF_6 is adsorbed only in the mesopores of the aerogel.

These surface fractal gels appear to be promising for a variety of applications. From the standpoint of heterogeneous catalysis, as the catalytic activity and transport efficiency are often dependent on surface self-similarity,[33] these gels could find use as efficient heterogeneous catalysts. The presence of palladium and cobalt metal centers in these gels strengthens their candidacy as catalysts. The porosity of these gels can be exploited to make gel-embedded filters to separate mixtures of gases based on the their differential adsorption propensities. The reversible adsorption of CO_2 can be harnessed practically by using these gels as CO_2 storage reservoirs.

Acknowledgment. Financial support for this research from NSF Grant CHE-0079169 is gratefully acknowledged. Professor George Scherer is thanked for insightful discussions and his generosity in making his laboratory equipment available to us.

CM034216M

(33) Kukovecz, A.; Konya, Z.; Palinko, I.; Monter, D.; Reschetilowski, W.; Kiricsi, I. *Chem. Mater.* **2001**, *13*, 345.